CONSERT constrains the internal structure of 67P at a few-metre size scale

Valérie Ciarletti, Alain Herique, Jérémie Lasue, Anny Chantal Levasseur-Regourd, Dirk Plettemeier, Florentin Lemonnier, Christophe Guiffaut, Pierre Pasquero, Wlodek Kofman

▶ **To cite this version:**

Valérie Ciarletti, Alain Herique, Jérémie Lasue, Anny Chantal Levasseur-Regourd, Dirk Plettemeier, et al.. CONSERT constrains the internal structure of 67P at a few-metre size scale. Monthly Notices of the Royal Astronomical Society, 2017, 469 (Suppl_2), pp.S805-S817. 10.1093/mnras/stx3132 . insu-01689580

HAL Id: insu-01689580
https://insu.hal.science/insu-01689580

Submitted on 11 Nov 2020

HAL is a multi-disciplinary open access archive for the deposit and dissemination of scientific research documents, whether they are published or not. The documents may come from teaching and research institutions in France or abroad, or from public or private research centers.

L'archive ouverte pluridisciplinaire **HAL**, est destinée au dépôt et à la diffusion de documents scientifiques de niveau recherche, publiés ou non, émanant des établissements d'enseignement et de recherche français ou étrangers, des laboratoires publics ou privés.

Monthly Notices
of the
ROYAL ASTRONOMICAL SOCIETY

MNRAS **469,** S805–S817 (2018)
Advance Access publication 2017 December 6

doi:10.1093/mnras/stx3132

CONSERT constrains the internal structure of 67P at a few metres size scale

Valérie Ciarletti,[1,2]★ Alain Herique,[3,4] Jérémie Lasue,[5] Anny-Chantal Levasseur-Regourd,[6] Dirk Plettemeier,[7] Florentin Lemmonier,[1,2] Christophe Guiffaut,[8] Pierre Pasquero[3,4] and Wlodek Kofman[3,4,9]

[1]*LATMOS/IPSL, UVSQ (Université Paris-Saclay), UPMC (Sorbonne Univ.), F-78280 Guyancourt, France*
[2]*CNRS, F-78280 Guyancourt, France*
[3]*IPAG, Université Grenoble Alpes, F-38000 Grenoble, France*
[4]*CNRS, IPAG, F-38000 Grenoble, France*
[5]*UPS-OMP, IRAP, Université de Toulouse, F-31400 Toulouse, France*
[6]*CNRS/INSU, LATMOS-IPSL, UPMC (Sorbonne Univ.), UVSQ (UPSay), F-75005 Paris, France*
[7]*Technische Universitat Dresden, Dresden, Sachsen, D-01062 Dresden, Germany*
[8]*XLIM, F-87060 Limoges, France*
[9]*Space Research Centre, PAN, Warsaw, PL-00-001, Poland*

Accepted 2017 November 28. Received 2017 November 20; in original form 2017 April 20

ABSTRACT

The internal properties of cometary nuclei are the best clues to the size distribution and properties of the early planetesimals that formed the planets during the early Solar system nebula processes. The CONSERT radar was designed to probe the interior of comet 67P/Churyumov–Gerasimenko with a wavelength of about 3 m. It was successfully operated during the First Science Sequence of the *Rosetta* mission when the CONSERT's wave propagated through part of the nucleus' small lobe. The shape of the received signals provides some hints about the internal structure of the comet's small lobe. The limited broadening observed on the received pulses is compared to simulations performed on a series of non-homogeneous nucleus models to put constrains on the potential structures at the wavelength's scale. The study allows to exclude structures showing a permittivity contrast larger than 0.25 inside the sounded part of the nucleus at a few metres size scale.

Key words: scattering – methods: numerical – techniques: radar astronomy – comets: general.

1 INTRODUCTION

The internal properties of cometary nuclei are the best clues to the size distribution and properties of the early planetesimals that formed the planets during the early Solar system nebula processes.

The CONSERT instrument was designed and developed to probe the interior of comet 67P/Churyumov–Gerasimenko (thereafter 67P/C-G) with a wavelength of about 3 m and to provide information about the internal structure of the nucleus. During the First Science Sequence (FSS) part of the small lobe of the nucleus was successfully sounded. The purpose of the work presented in this paper is to find constrains on the internal structures in terms of size and composition at a scale commensurate with the wavelength.

To this aim, the shape on the received pulses is compared to numerical simulations performed on a series of non-homogeneous nucleus models.

2 COMET 67P/C-G CONTEXT

2.1 Low density of cometary nuclei

Before *Rosetta*'s rendezvous with comet 67P/C-G, the bulk density of its nucleus, as for other comets, had been estimated from its mass, derived from non-gravitational forces and from its size, tentatively estimated from remote observations in the visible and the infrared. It was found to be very low with an upper limit around 500 kg m^{-3} (Davidsson & Gutiérrez 2005), quite typical of most cometary nuclei densities (Weissman & Lowry 2008). Such a result indicates a nucleus structure dominated by voids, suggesting the presence of fractures and possible sub-nuclei structures, together with an intrinsic micro-porosity of the nucleus' ices and

★ E-mail: valerie.ciarletti@latmos.ipsl.fr

© 2017 The Author(s)
Published by Oxford University Press on behalf of the Royal Astronomical Society

Downloaded from https://academic.oup.com/mnras/article/469/Suppl_2/S805/4705912 by guest on 11 November 2020

refractories, in agreement with clues from the structure of dust particles in the coma (Levasseur-Regourd et al. 2009). Early after the *Rosetta* rendezvous, the bulk density of 67P/C-G was estimated to be about (470 ± 45) kg m^{-3}, through RSI and OSIRIS determinations of, respectively, the mass and the shape (Sierks et al. 2015). Once the Southern hemisphere was illuminated and the global shape determined, results would converge towards a more precise value of (533 ± 6) kg m^{-3} (Pätzold et al. 2016) or of (532 ± 7) kg m^{-3} (Jorda et al. 2016). These final results strongly confirm the large porosity (70–80 per cent) estimated for the nucleus, which needs to be explained by either micro or macro porosity structures.

2.2 Cometary nuclei interior structure

Because of their high volatile content and short lifetime in the inner Solar system, cometary nuclei have long been argued to be the most pristine remnants of early Solar system accretion processes beyond its inner water condensation limit. *Rosetta*'s recent measurements at comet 67P/C-G during more than 2 yr along its trajectory, before and after perihelion, correspond to major improvements of our understanding of cometary evolution. On the one hand, they clearly indicate the pristine state of the comet from the detection of very volatile species (N_2 and O_2; Bieler et al. 2015; Rubin et al. 2015) indicating an internal temperature between 30 and 40 K. They also provide evidence for (as already mentioned) a very low density of the nucleus of about 530 kg m^{-3}, for a limited aqueous alteration (Davidsson et al. 2016), and for pristine fluffy dust particles with very low densities, typical of hierarchical structures, at least from tens of nanometres to tens of millimetres, and fractal dimensions close to 2, probably remnants of the initial accretion of this small body. Such conclusions were provided by GIADA, MIDAS, and COSIMA dust measurements (Fulle et al. 2015; Bentley et al. 2016; Langevin et al. 2016; Mannel et al. 2016). On the other hand, they highlight the vigorous resurfacing processes at work during the activity phases of the comet near the Sun, as expected from thermophysical properties of cometary nuclei materials (De Sanctis et al. 2010). This is illustrated by the occurrence of multiple sporadic outbursts and jets (Sierks et al. 2015; Vincent et al. 2015; 2016; Grün et al. 2016), the loss of material equivalent to a global 1 m depth erosion mostly located in the Southern hemisphere where icy patches are subsequently observed (Bertaux 2015; Groussin et al. 2015; Pommerol et al. 2015; Filacchione et al. 2016) and finally the associated dust transport and deposition from the Southern to the Northern hemisphere (Thomas et al. 2015a,b). Because its activity systematically resurfaces the comet, the clues linked to the formation processes of the body have to be probed through the physical properties of the material at depth.

Trails of debris have been detected along cometary orbits for many Jupiter Family comets, including 67P/C-G), mostly from infrared remote imaging (Kelley, Reach & Lien 2008; Agarwal et al. 2010). Catastrophic disruptions or partial fragmentation events serendipitously offer the possibility to detect some cometary nuclei internal properties. Indeed, such events can lead to the release of evaporating icy fragments from the nucleus with sizes up to a few tens to hundreds of metres (e.g. Asphaug & Benz 1996; Desvoivres et al. 2000; Levasseur-Regourd et al. 2009). The fragments released in such events might correspond to the internal building blocks of the nucleus, and to some extent to parts of a surficial crust. As comets are varied objects with few hints to potential chemical composition taxonomies (see e.g. Mumma & Charnley 2011), it is most likely that the interior of nuclei cover a range of physical and chemical properties depending on their region of formation and their subsequent evolution. Many fragmentation events have been observed but there are no particular patterns to predict comet splitting (for a review, see Boehnhardt 2004; Fernández 2009). In general, the secondary nuclei are observed to present tails, comae, and activity similar to single nuclei. The spectacular observations of the breakup of comet 73P/Schwassmann–Wachmann 3 in 2006 demonstrated that the size distribution of the ejected fragments could be fitted with a differential power law of coefficient −3.34 (Ishiguro et al. 2009; Reach et al. 2009), a coefficient similar to populations of planetesimals in collisional equilibrium (e.g. Hellyer 1970). Spectroscopic observations of the above-mentioned comet indicate no strong differences in composition between the fragments (Dello Russo et al. 2007; Schleicher & Bair 2011), though clues to possible differences in the dust properties, which might give an insight on different properties of inner sub-nuclei, were noticed (Hadamcik Levasseur-Regourd 2016). These observations could be consistent with the hypothesis that cometary nuclei fragments represent primordial blocks of the accretion of comets.

2.3 Variety of structures detected on the surface of 67P/C-G

The OSIRIS experiment on-board *Rosetta* has revealed the surface of the nucleus to be more complex than could be assumed from previous missions, from larger distances and through fast flybys (Sierks et al. 2015; Thomas et al. 2015a). A wide variety of structures has been discovered, with pits and depressions (both quasi-circular structures ranging from about 50 to 200 m in diameter), as well as boulders, terraces, cracks, and fractures, possible impact craters and dune morphologies. The distribution of various features within different regions of the nucleus is detailed in table 2 of El-Maarry et al. (2015).

Pits, with a depth/diameter ratio near 1, happen to be in some cases the sources of nucleus activity and reveal on their walls repeating structures with a typical scale of 3 m (Sierks et al. 2015). These pits may be clues to large (several tens of metres) heterogeneities in the structural properties of the nucleus below the surface. They could either have formed from sinkhole collapse, meaning that voids might have existed in the nucleus since its formation or result of internal heat changes, then only existing close to the surface (Vincent et al. 2015). Depressions present flat floors and walls indicating a consolidated structure, and might result from endogenic processes or impacts (Auger et al. 2015).

At the surface of 67P/C-G, boulders are present with sizes in the 1–100-m range. They are mainly found on gravitational slopes lower than 35° and could be erosion products (Auger et al. 2015). Their size–frequency distributions were noticed to be similar in alike geomorphological regions and are thus estimated to be due to similar processes (Pajola et al. 2015). While the inner structure of these boulders is unknown, it may be of interest to notice that a few large solid chunks have been observed by OSIRIS in the inner coma (e.g. Rotundi et al. 2015). Ejection of these decimetre-sized objects (before perihelion) could be a clue to a density substantially below the nucleus bulk value, and thus of an extremely high porosity (Davidsson et al. 2015). The global distribution of boulders on the surface of comet 67P/C-G is certainly shaped by sublimation and erosion processes (Pajola et al. 2015). However, observations of lumpy features on dust-free 67P/C-G surfaces, such as rounded nodules, so-called goose bumps, located on the walls of large and deep pits in the Seth region discussed in Sierks et al. (2015); their size distribution is centred around 2–3 m, and they have been argued to represent a signature of the primordial building blocks of 67P/C-G (Davidsson et al. 2016). If this is the case, then the

Downloaded from https://academic.oup.com/mnras/article/469/Suppl_2/S805/4705912 by guest on 11 November 2020

cometesimals would have presented a population of bodies with a monodisperse size distribution of about 3 m.

In situ observations of 9P/Tempel 1 during Deep Impact mission and of 67P/C-G during the *Rosetta* mission have shown the presence of geological 'layers' or terraces on their surfaces (Thomas, Alexander & Keller 2008; Ciarletti et al. 2015; Massironi et al. 2015). They indicate an inner stratification, which could result from sublimation or be primordial. Some authors have suggested that cometary layering may reflect a primordial accretion processes. Layering processes at the formation of comets could originate from the deformation of large accreting cometesimals during collisions (Belton et al. 2007; Jutzi & Asphaug 2015), from collision induced sintering on cometesimals aggregates (Lasue et al. 2009, 2011), or from pebble accretion that coalesced in streaming instabilities within the turbulent protosolar nebula (Johanssen et al. 2007; Wahlberg Jansson & Johansen 2015). In this context, cometesimals are understood as the smallest sized bodies that formed in the early Solar system and coalesced to form the cometary nuclei. Their typical sizes range from pebbles of a few millimetres to centimetres, to cometesimals of 10–100 m (e.g. Weidenschilling 2004; Johansen et al. 2015). Whether 67P/C-G has retained its main characteristics of a bilobate shape, with the presence of layers and cracks, volatiles in the interior, and limited aqueous alteration since the beginning of the Solar system as a primordial body (e.g. Davidsson et al. 2016) or if it is a later rubble-pile object formed by reaccretion of cometary fragments (e.g. Morbidelli & Rickman 2015; Rickman et al. 2015) remains a matter of debate.

2.4 Nucleus composition and realistic range of permittivity values

To shed light on the particular processes at work during 67P/C-G's accretion, it is necessary to assess the internal structure of the comet nucleus at depth and the size distribution of inhomogeneities that could represent cometary building blocks, should they be present. This was the goal of the CONSERT radar, which probed the small lobe of 67P/C-G to depths of a couple of 100 m during the FSS. The initial analysis of the CONSERT signal indicates that the bulk cometary material has a very low relative dielectric permittivity of 1.27 ± 0.05 through the parts of the small lobe that have been sounded by the experiment in the vicinity of Philae's landing site (Kofman et al. 2015).

In this work, we look more closely at the CONSERT signal travelling through different parts of the small lobe, and use numerical simulations of the signal's propagation to constrain the properties of heterogeneities that may be present inside the nucleus. Since the propagation of the electromagnetic waves is essentially driven by the dielectric permittivity of the medium, CONSERT data provide first-hand information about the permittivity value and its variability inside the sounded volume of the nucleus.

At low temperatures, in the 90–150 K range at the landing site of Philae (Spohn et al. 2015; Lethuillier et al. 2016), and certainly around 30–40 K inside the nucleus as argued in Section 2.1, the permittivity weakly depends on temperature (e.g. Heggy et al. 2012). Therefore, the range of permittivity to be considered for the cometary material mostly depends on the porosity and/or composition of the material.

We know that comets' nuclei are mixtures of materials with a high porosity (more than 75 per cent in the case of 67P/C-G), ices (mainly H_2O, CO_2 and CO) and refractory dust particles (typically minerals and organic compounds) as they are detected in the coma of comets from ground-based observations and *in situ* measurements (e.g. Cochran et al. 2015; Wright et al. 2015; Altwegg et al. 2016; Fray et al. 2016). At CONSERT's 90 MHz frequency and at low temperature, the permittivity values for non-porous ices range from 3.1 to 3.4 for H_2O hexagonal and amorphous ices, around 2.1 for CO_2 ice and around 1.4 for CO ice (Hérique et al. 2016 and references therein). The values for refractory materials are less easy to determine because intrinsic micrometre-scale porosity is always present. Nevertheless, some values can be found in the literature for meteorites measured in the laboratory (Heggy et al. 2012; Hérique et al. 2016) or for minerals and carbonaceous compounds relevant to cometary materials, which may vary from a low 2 for pure refractory carbon up to around 7 for Mg-silicates minerals (for a review see table 7 in Hérique et al. 2016, and Brouet et al. 2016).

For a given mixture of materials, mixing formulas provide an estimated range for the resulting permittivity value. But retrieving the composition of a mixture from its measured permittivity value is challenging since a given permittivity value can be obtained by a huge number of mixtures. However, it provides constraints on the composition especially when combined with information from other instruments. An efficient approach is to test possible scenarios for the dust fraction composition. This approach has been used to interpret the 1.27 ± 0.05 permittivity value inside the small lobe of 67P/C-G from CONSERT's data (Kofman et al. 2015): in combination with the density from RSI and the dust to ice ratio from GIADA and ROSINA measurements, the bulk porosity value as estimated by CONSERT is about 75 per cent in volume, a value in agreement with previous *in situ* cometary dust studies at comet 1P/Halley (Jessberger, Christoforidis & Kissel 1988), with analyses of micrometeorites possibly of cometary origin collected on the ground (Engrand & Maurette 1998; Flynn et al. 2016) and with more recent COSIMA dust mass spectrometer measurements at 67P/C-G (Fray et al. 2016). Then, Hérique et al. (2016) improved this interpretation and showed that the permittivity value for the refractory dust cannot be very large, which is only consistent with a major contribution from carbonaceous material in the dust fraction of 67P/C-G's cometary material.

3 ANALYSIS OF THE SHAPE OF THE CONSERT RADIO PULSES

CONSERT is a bistatic radar designed to characterize the nucleus internal structure. To achieve this objective, transmitters and receivers operating at a central frequency of 90 MHz (equivalent to a wavelength of 3.3 m in vacuum) are accommodated on board both the *Rosetta*'s main spacecraft (hereafter the orbiter) and Philae. The instrument, described in detail in Kofman et al. (1998, 2007), has been successfully operated during the mission. CONSERT's data have been acquired in three different contexts and configurations (Kofman et al. 2015): (1) when Philae was separated from the main spacecraft but not yet in contact with the nucleus during the Separation Descent Landing (SDL) phase, (2) during the FSS after Philae landing at Abydos (which is the name given to the location of Philae's landing site) and when the CONSERT waves propagated through parts of the smaller lobe of the nucleus, and finally (3) after the FSS, when Philae at Abydos was in line of sight with *Rosetta*'s main spacecraft in order to constrain Philae's location by triangulation (Hérique et al. 2015).

The work presented in this paper relies on data acquired during the FSS, which are the only ones corresponding to actual propagation through parts of the small lobe of the nucleus and sounding the cometary material. The quantitative interpretation of these FSS CONSERT's data is complicated by the bistatic configuration

Downloaded from https://academic.oup.com/mnras/article/469/Suppl_2/S805/4705912 by guest on 11 November 2020

around a surface with an intricate topography, and the fact that the position and orientation of the CONSERT's antenna on Philae are far from being nominal, as finally confirmed in early September 2016 when Philae was eventually seen on 67P/C-G's surface (http://www.esa.int/Our_Activities/Space_Science/Rosetta/Philae_found). Therefore, the interpretation of the CONSERT's observations is not straightforward but relies on the comparison of experimental data with synthetic data, with a view to constraining the physical parameters of the propagating material from the time delay, intensity, and deformation of the transmitted signal (e.g. Richards 2005). The synthetic data are obtained from numerical simulations relevant to the propagation of the CONSERT instrument's signal through a parametric model of the nucleus, chosen to explore the physical parameters we want to constrain. These physical parameters correspond to the dielectric permittivity range of the cometary material as detailed in Section 2.4, the typical size of the internal structures within the cometary material and the length of propagation through this material.

This method has provided the first estimate of the mean permittivity inside the volume of the small lobe of the nucleus actually sounded by CONSERT (Kofman et al. 2015). In that case, ray-tracing simulations were performed assuming a homogeneous nucleus and taking into account the refraction of the wave across the nucleus' surface. The simulated delays were compared to the measured ones on both directions probed by the sounding (West and East of Abydos), which behaved in opposite ways. The combination of simulations on many possible positions of Philae on the surface of 67P/C-G led to a relatively precise estimated value of the mean dielectric permittivity of 1.27 ± 0.05 (Hérique et al. 2016) and, at the same time, constrained the location of Philae inside an area of 22.6×41.5 m^2 (Hérique et al. 2015). It was further determined from the shape of the radio wave peak signal that the cometary material was very weakly dispersive, giving support to the hypothesis of a homogeneous cometary material, at least down to the scale of the wavelength, of about 3 m (Kofman et al. 2015).

In this work, we focus on assessing the potential presence of heterogeneities at a scale of the order of a few metres. Following the above-mentioned method, experimental data are compared to simulated ones in order to exhibit constraints on the spatial scale and the permittivity contrast of heterogeneities inside the sounded volume, which can be compatible with CONSERT's data.

3.1 The radio wave pulses shape parameters

It is possible to characterize the CONSERT's signal by a few parameters chosen to efficiently analyse the effect of the propagation, namely: the propagation delay, the width and amplitude of the received pulse, and the number of received pulses. The propagation delay was already used, as mentioned, to retrieve the real part of the permittivity mean value (Kofman et al. 2015; Hérique et al. 2016) and to provide an estimate of Philae's location (Hérique et al. 2015). Now that the precise position of Philae has been determined, work is on-going to characterize potential differences in the time delay between the Western and Eastern sounded regions, which would indicate differences, if any, in dielectric properties for different regions of the small lobe of 67P/C-G.

Further analysis of the received amplitude is on-going. It requires a much more complex analysis that needs to take into account the location of both the receiver and the transmitter, the nucleus shape, the orientation of Philae's antennas – impacting the polarization of the transmitted waves – and an accurate description of Philae's close environment – impacting Philae's antennas radiation pattern (Plettemeier et al. 2016).

For the purpose of our study, we chose to focus on the shape of the received pulses since the width of these pulses is likely to be linked to the level of heterogeneity inside the sounded volume of the nucleus.

3.2 CONSERT radio pulse width estimation and calibration

When a radio wave propagates through a non-homogeneous medium, volume scattering can be responsible for waveform spreading, provided that the permittivity spatial variation is large enough and that the scale of the heterogeneities is commensurate with the wavelength. To study and quantify this potential spreading on the data, we need a reliable baseline reference corresponding to propagation through a homogeneous medium. Deviation from this reference would be an indication of possible scattering and can be compared to simulated data to characterize the propagation medium.

3.2.1 Measuring the pulse width from CONSERT *data*

CONSERT is an instrument designed to characterize the propagation's conditions between Philae and the orbiter. An in-time transponder structure has been developed to bypass the clock accuracy limitations and achieve an accurate time delay measurement as described in several papers (e.g. Kofman et al. 1998, 2007; Hérique et al. 2015). The actual signal used by CONSERT is a BPSK-coded (Binary Phase Shift Keying) sequence at a rate of 10 symbols per μs (corresponding to a frequency bandwidth around 10 MHz). This sequence is modulated at 90 MHz to be transmitted and received by the antennas. The receiver's frequency bandwidth is around 8 MHz, thus slightly narrower than the signal frequency bandwidth leading to an expected pulse width around 0.125 μs. After demodulation in phase and in quadrature, the received signal is sampled at 10 MHz. This sampling frequency is close to the Nyquist frequency but still lower than the theoretically needed value, the induced aliasing is limited but specific caution must be taken to interpolate the signal on-ground and compensate the transponder effects, in order to accurately retrieve the propagation delay and estimate the pulse spreading.

A dedicated on-ground processing has thus been developed to produce properly compressed by model and interpolated CONSERT's pulses (Pasquero, Herique & Kofman 2017). It has been tested and validated on a calibration data set obtained on the ground with CONSERT's electronics spare models, where the homogeneous propagation medium was simulated by coaxial cables and attenuators. It is implemented in the CONSERT signal-processing pipeline and applied to retrieve the propagation delay on the SDL and FSS signals for both science and operational purposes (Hérique et al. 2015; Kofman et al. 2015). To estimate the width of the received pulses, we use the signal interpolated, as explained above in order to avoid bias introduced by classical interpolation methods like Fourier interpolation that are not adapted to partially aliased signals. Two parameters have been used for the study (see Fig. 1): the pulse width at 3 dB ($\Delta T_{3\mathrm{dB}}$) and at 6 dB ($\Delta T_{6\mathrm{dB}}$) for the maximum value. Despite the fact that the compressed-by-model data processing was initially designed to obtain an improved estimate of the propagation delay, we are confident that it also provides relevant pulse width values.

Downloaded from https://academic.oup.com/mnras/article/469/Suppl_2/S805/4705912 by guest on 11 November 2020

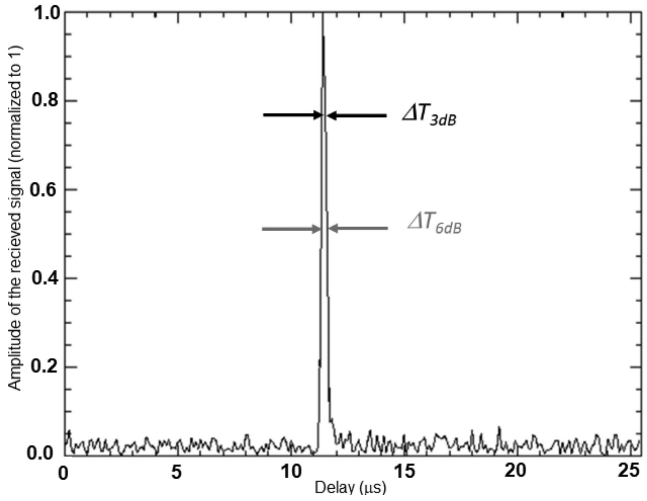

Figure 1. Typical shape of an experimental normalized CONSERT's pulse and definition of the pulse widths $\Delta T_{3\mathrm{dB}}$ and $\Delta T_{6\mathrm{dB}}$. In this case the pulse widths are determined to be 0.13 and 0.18 μs.

3.2.2 Baseline reference value for the pulse width

The precise shape and width of the pulse that would be received after propagation through a perfectly homogeneous medium depends on the transfer function of the transmitters, receivers and antennas in the direction of the wave propagation.

It cannot be experimentally obtained using data collected when Philae and *Rosetta* were in line-of-sight during the SDL or, even better with Philae on 67P/C-G nucleus, when some additional direct transmissions have been performed to get an estimate of Philae's location by triangulation during FSS. Indeed, for these two configurations, the transmission between Philae and the Orbiter was established in effective directions quite different from the one used during FSS with respect to the antennas' main lobe principal direction. Since the antennas' radiation pattern is frequency dependent, the distortion induced by the antennas in one direction can differ significantly from the one observed in another direction. As a consequence, these two sets of data cannot be used as a reference for the analysis of the FSS data.

In 2002, before launch, CONSERT radar electronics had been calibrated on the ground in relevant thermal conditions, with electronics connected with coaxial cables. A calibration data set provides reference pulse width in absence of scattering. These reference measurements do not take into account potentially less important instrumental effects such as electronic aging, temperature variability, and the antenna distortion from pattern and matching network. We are also aware that the potential impact of the nucleus on the radiation pattern of the antennas is not accounted for in these measurements. Nevertheless, they provide a reliable enough basis for the experimental and simulated data interpretation.

The pulse widths due to the limited frequency bandwidth of the electronics units (including both the receivers and transmitters) $\Delta T_{\mathrm{ref3dB}}$ and $\Delta T_{\mathrm{ref6dB}}$ have been computed on a data set of 7000 measurements performed with a very good signal-to-noise ratio (SNR; >40 dB). The histograms of the measured obtained values are show in Fig. 2. The obtained mean values are $\Delta T_{\mathrm{ref3dB}} = 0.113$ μs with a standard deviation of 0.007 μs and $\Delta T_{\mathrm{ref6dB}} = 0.152$ μs with a standard deviation of 0.024 μs. The widths measured at 3 and 6 dB are coherent (for a perfect compressed BPSK, $\Delta T_{\mathrm{ref6dB}}/\Delta T_{\mathrm{ref3dB}}\sqrt{2}$). The dispersion increases significantly when we consider the pulse width at 6 dB which corresponds to the oscillations from the imperfect compensation of the aliasing (see Pasquero, Herique & Kofman 2017, fig 10).

As previously mentioned, after Philae rebounds during the SDL, CONSERT was operated with a lander in a far-from-nominal attitude. The antenna pattern which results in the coupling of the CONSERT monopole antennas with the lander body and the nucleus likely environment, has been significantly impacted by this uncontrolled geometry. Initial electromagnetic simulations of this complex configuration have been performed. They take into account the Digital Terrain Model of the landing site determined from the OSIRIS data (Capanna et al. 2016), the permittivity value estimated by CONSERT and the recently confirmed attitude of Philae and its antennas. As expected, preliminary results show that a limited pulse broadening is indeed likely to take place (Plettemeier et al. 2017).

Only the analysis performed on the $\Delta T_{6\mathrm{dB}}$ values is presented in this paper. The observed trends are confirmed by the analysis of the $\Delta T_{3\mathrm{dB}}$ values.

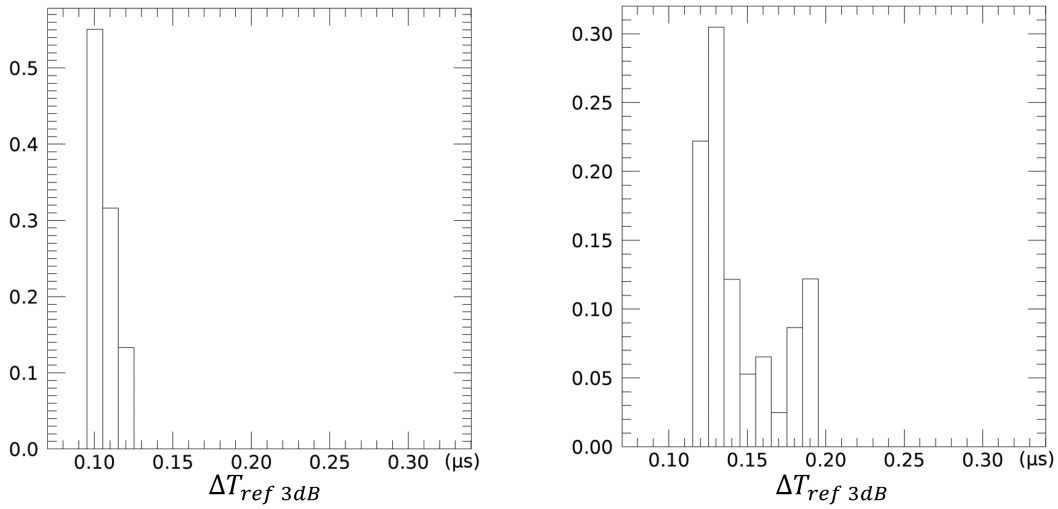

Figure 2. Histograms of the pulse widths due to the electronics at 3 dB (left) and 6 dB (right) computed on 7000 measurements (number of occurrences normalized by the total number of analysed sounding).

Downloaded from https://academic.oup.com/mnras/article/469/Suppl_2/S805/4705912 by guest on 11 November 2020

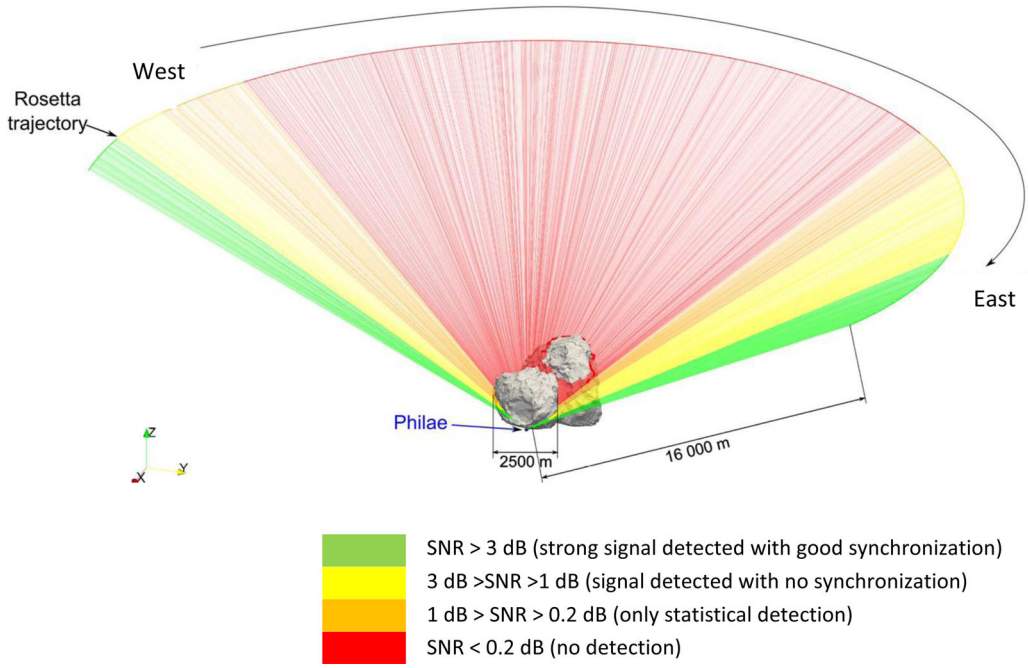

Figure 3. FSS configuration, adapted from Kofman et al. (2015). The approximate dimension of the nucleus' small lobe is indicated as well as the typical distance between Philae and *Rosetta* during FSS. In this paper, only signals corresponding to a strong enough SNR (i.e. corresponding to the green and yellow lines) have been used.

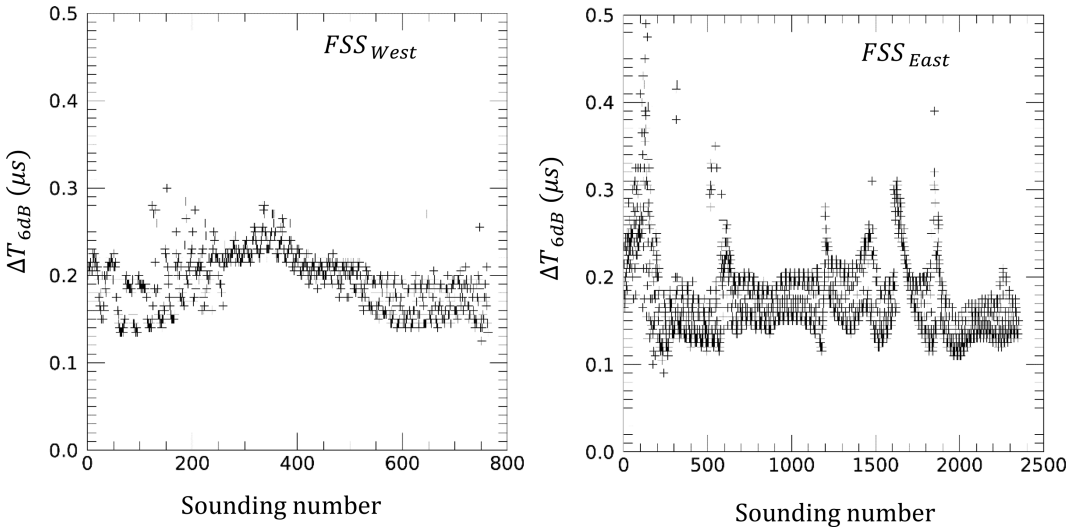

Figure 4. Pulse widths at 6 dB $\Delta T_{6\mathrm{dB}}$ measured during FSS as a function of the sounding number for FSS_{West} (left) and FSS_{East} (right).

3.3 Calculated width of CONSERT's pulses obtained through the comet during FSS

During FSS, soundings have been successfully performed through parts of the small lobe between Philae and *Rosetta*. Fig. 3 shows the location of Philae at Abydos and the trajectory of the main spacecraft during FFS. For each sounding, the colour used for the straight line that connects Philae and *Rosetta* is representative of the SNR value. The green (SNR > 3 dB) and yellow (3 dB > SNR > 1 dB) colours represent correct signal detections and provide the data set used for the present study.

Therefore, two distinct sets of data with a sufficient SNR are considered in the following: FSS_{West} corresponding to measurements performed when *Rosetta* was located West of Abydos in the early part of the CONSERT measurement sequence and FSS_{East} when *Rosetta* was East of Abydos during the final part of the CONSERT measurement sequence.

A preliminary work made on the estimation of the distances actually travelled inside the nucleus during FSS show that the distances are globally increasing during FSS_{West} and decreasing for FSS_{East} but remaining between 900 and 200 m.

As previously explained, the pulse widths of the FSS measurements are computed to be quantitatively analysed and compared to the calibration values. For both FSS_{West} and FSS_{East}, the experimental values of $\Delta T_{6\mathrm{dB}}$ are displayed as a function of the sounding number in Fig. 4, the corresponding histograms are shown in Fig. 5.

These ΔT values present quite obvious regular oscillations with an amplitude around 0.05 μs, which can simultaneously be

Downloaded from https://academic.oup.com/mnras/article/469/Suppl_2/S805/4705912 by guest on 11 November 2020

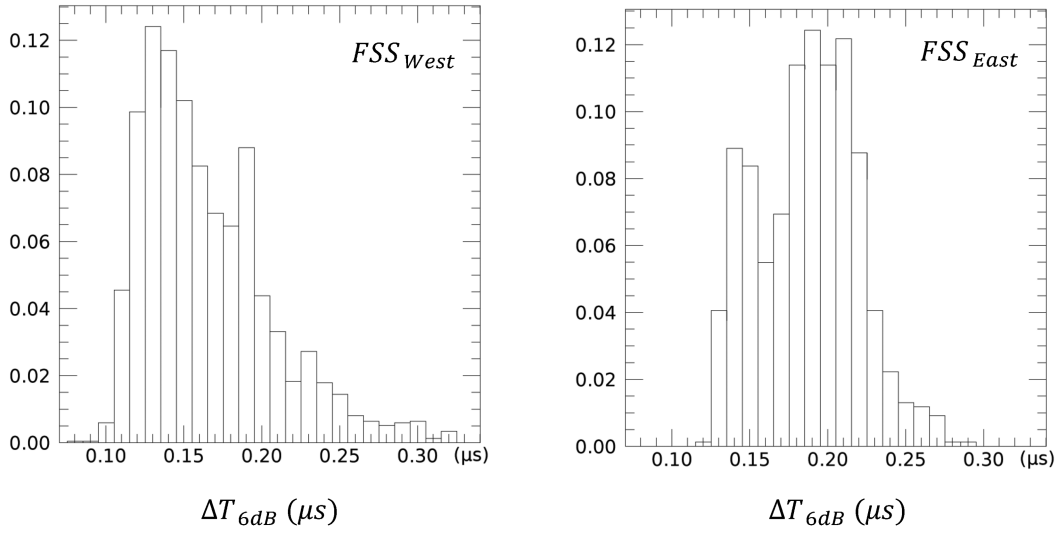

Figure 5. Histograms (number of occurrences normalized by the total number of analysed soundings) of the ΔT_{6dB} values for FSS_{West} (left) and FSS_{East} (right) presented as a function of the sounding number in Fig. 4.

Table 1. Pulse width values at 6 dB.

	ΔT_{6dB} (μs)		
	Mean	Std	Mean + Std
Reference	0.152	0.024	0.176
FSS_{West}	0.194	0.032	0.226
FSS_{East}	0.174	0.048	0.222

observed on the amplitude of the received pulses too. This periodic phenomenon, which is not visible on the calibration data or on the cruise measurements, is still under study. But, given its persistence and regularity throughout the whole FSS acquisition sequence, a geophysical origin inside the nucleus can be straightaway excluded. An instrumental origin is being considered for this oscillation especially the distortions from antenna patterns and some possible multipath propagation at orbiter level.

The mean ΔT_{6dB} values computed on the FSS_{West} and FSS_{East} with their standard deviation (Std) are given in Table 1. They show, as expected, a slight broadening of the pulse widths during FSS with respect to the ground calibration values, ΔT_{ref}. The discrepancy with the reference values is quite small and might not be significant if we consider the effects of the sampling rate mentioned above.

The ΔT FSS data present some very limited areas with larger values but the corresponding signals do not present any features characteristic of volume scattering, i.e. increase of the effect with the distance travelled inside the nucleus and asymmetric pulse shape with a trail at the right of the maximum. The higher values at the beginning of FSS_{East} (around position #150 Fig. 4 right) have been collected with a degraded SNR (<15 dB) that explains the enlargement of the pulse. The observed sporadic occurrences of peak enlargement during FSS_{East} are very limited in time and associated with fast phase rotation which is characteristic of interferences likely due to surface topography.

In conclusion, the CONSERT's signal does not present any evidence of significant scattering through the cometary material, as determined earlier. In the next section, we compare the peak widths values measured on CONSERT's signal to wave propagation numerical simulations to constrain the level of inhomogeneity inside the nucleus that would be compatible with the observations.

To obtain an experimental pulse width value for comparison with the simulated data, we chose to use the mean ΔT value augmented by its standard deviation (see Table 1). Even if some slight differences can be noticed between FSS_{West} and FSS_{East}, we consider, for the results presented here, a unique threshold experimental ΔT_{FSS} value for the whole FSS measurements $\Delta T_{FSS6dB} = 0.226\ \mu$s for the pulse width at 6 dB (see Table 1). In the following discussion, simulated pulse width values above these thresholds are considered not to be in agreement with the FSS data.

4 SIMULATION OF ELECTROMAGNETIC WAVE PROPAGATION THROUGH INHOMOGENEOUS MATERIALS

4.1 Numerical method

We have selected the Finite Difference Time Domain (FDTD) method (Taflove & Hagness 2005) to model the wave propagation in the nucleus material. The FDTD method is a numerical method widely used in electromagnetic simulations. Compared to other methods operating in the frequency domain, which may run faster, it offers definite advantages for our problem. First, it is based on a rigorous formulation and solves directly the set of Maxwell equations without any physical approximation. Secondly, it is a versatile method quite easy to implement and the accuracy of the numerical scheme can be controlled by the time-steps or grid spacing. Working in the time domain is clearly an advantage since the exact waveform transmitted by the antenna is used as the input signal and subsequent propagation and scattering of the waves can be followed in a straightforward manner. Finally, it is a three-dimensional approach which allows us to take into account heterogeneities of the electromagnetic properties inside the nucleus down to the scale of the spatial mesh. Besides, increasing the heterogeneity of the propagation medium does not change the computational or memory costs.

To obtain reliable simulated data, the size of the FDTD cells must be small enough to correctly describe the way the wave propagates through it. The required condition commonly used is for the mesh grid spacing, Δ, to be smaller than one tenth of the wavelength in

Downloaded from https://academic.oup.com/mnras/article/469/Suppl_2/S805/4705912 by guest on 11 November 2020

the medium. For our study, the mean permittivity value is set to 1.27 in agreement with CONSERT's inferred average bulk permittivity value and we consider local values ranging from 1 (vacuum) to 2 (determined for nearly pure dust organic compounds as specified in Section 2.4). Therefore, Δ can be set to 0.2 m for each of the three spatial dimensions. Tests have been performed to check that this value is small enough to give accurate results on well-known cases.

A consequence of the small Δ value is that the volume of the whole nucleus (about 21.4 km^3, Sierks et al. 2015) cannot be discretized with such a small spacing. In fact, it would lead to a number of FDTD cells around 10^{30}, which would require unrealistic computational resources. Therefore, we need to reduce the volume used for the simulations while keeping it relevant to the phenomena we are interested in for the study, i.e. the potential effect that heterogeneities of a few metres size would have on CONSERT's pulse width. We thus model the 3D propagation of CONSERT's pulse in limited but still significant computational volumes equal to ($100 \times 100 \times L$) cubic metres, L being the distance propagated through the nucleus in metres. We are aware that this precludes any conclusion that would be linked to the nucleus shape and that we exclusively focus on the effect of the small-scale heterogeneities. This reduction can be justified if the limited volume is still statistically representative of the parameters of the nucleus model, specifically if the size of the heterogeneities is small compared to the volume's dimensions. The size chosen for the computational volume allows us to simulate heterogeneities with characteristic dimensions in the 0.2–10-m range.

We use the FDTD solver TEMSI-FD (Guifaud and Reineix, 2016). It includes suitably absorbing boundary conditions with Perfectly Matched Layers (Bérenger 1994), to eliminate the parasitic reflexions that occur at the limit of the finite computational volume. It also provides adequate fractal models to simulate non-homogeneous environments.

4.2 Cometary small-scale structure models

Our purpose is to investigate the effect of potential heterogeneities of a few metres size inside the nucleus. In order to minimize a model-dependent bias, we choose to consider two types of structures generated by two random processes as different as possible: a band-limited fractal model suitable to simulate sponge-like internal structures and related micro porosities, and a model based on spheres of the same size embedded in a homogeneous host matrix, which may be relevant in the case of aggregated cometesimals as described in Section 2.2. Given the high porosity value and the materials that are anticipated for the nucleus composition, the geophysical parameter that is considered in the study is the real part of the relative permittivity value, simply noted, ε, hereafter. Each nucleus model considered for the study has a global permittivity value of 1.27 ± 0.05 (computed on the velocity of the waves) to be in agreement with the mean permittivity estimated from CONSERT's propagation delay. The second physical parameter that impacts the wave propagation through the material is the scale of the heterogeneities inside the cometary material. How we vary these two parameters in the simulations is explained in the following sections.

4.2.1 Diamond-square fractal structure

For this first model, we chose to generate heterogeneities inside the nucleus using a fractal model that can easily allow us to study the impact of the size of the heterogeneities and the permittivity contrast on the way the CONSERT's waves propagate through it. Fractal models are commonly used to model non-deterministic natural patterns that show self-similarity over extended but still finite scale ranges e.g. river network, coastlines, surfaces, clouds, etc. (Mandelbrot 1977). It is also generally recognized that low velocity accretion of solid matter in the gas environment of the protosolar nebula leads to the formation of low density fractal aggregates with irregular shapes that could be representative of cometary nuclei (Donn 1990). Internal variations of composition, density or cohesive strength are expected to result from the accretion process (Donn 1990; Lasue et al. 2009, 2011) and could translate into fractal variations of the dielectric constant inside the nucleus. The idea of a fractal structure inside the nucleus is supported by observations made at the surface at Philae's landing site and within the innermost coma. Comet Infrared and Visible Analyser (CIVA)'s images revealed a very fractured surface with complex structure and a variety of grain scales and albedos (Poulet et al. 2016) and Rosetta Lander Imaging System images showed a surface with a bi-modal brightness distribution which has been interpreted in terms of degree of consolidation suggesting that the surface below the lander could consist of smooth, cracked plates with unconsolidated edges, similar to terrain seen in CIVA images (Schröder et al. 2017). Besides, dust experiments on-board *Rosetta* strongly suggested that the dust particles present a fractal hierarchical structure (Fulle et al. 2015; Bentley et al. 2016; Mannel et al. 2016).

Building a fractal model requires an elementary pattern and a rule to split the pattern or to transform it usually by self-similarity in an iterative process. The algorithm proposed by TEMSI-FD is based on the diamond-square splitting technique (Miller 1986) that is described in the on-line supplementary material. We choose to describe the 3D fractal structures obtained (see illustration in Fig. 6a) by the two most relevant parameters: the spatial scale d_{frac} (corresponding to the typical size of the larger structures generated by the method) and the permittivity contrast $\Delta\varepsilon = \varepsilon_{\max} - \varepsilon_{\min}$, whose values can be linked to physical models of the nucleus. The statistical variability of the models characterized by the same d_{frac} and $\Delta\varepsilon$ is integrated in the results shown in the following through the standard deviation of the computed pulse width.

4.2.2 Spheres-based structure

This second model is constituted by a number of spheres of the same diameter value (d_{sph}) randomly distributed inside the computational volume. The choice has been made to allow overlapping spheres, which results in possibly larger structures consistent with low collision and accretion processes of the spheres (see Fig. 6b). The spheres and the matrix host are characterized by two different permittivity values. The size of the spheres is taken as the heterogeneity size relevant for CONSERT measurements comparison.

4.3 Simulated CONSERT data

A number of simulations have been performed for the fractal and the spheres models that represent two as different as possible spatial structures for the nucleus. For each structure, we focus on two integrated parameters a spatial scale (d_{frac} or d_{sph}) ranging from 0.6 to 8 m and a permittivity contrast $\Delta\varepsilon$ ranging from 0 (homogeneous material) to 0.8.

For each considered internal structure scale and permittivity contrast $\Delta\varepsilon$, we simulate the propagation of the pulse through 60 different realizations of the same random process to obtain statistically

Downloaded from https://academic.oup.com/mnras/article/469/Suppl_2/S805/4705912 by guest on 11 November 2020

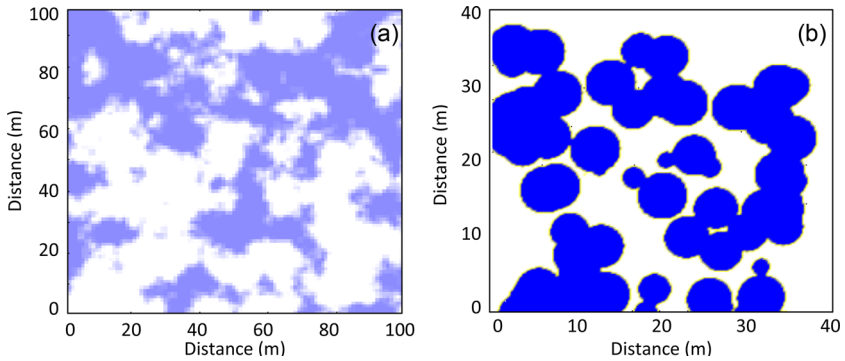

Figure 6. 2D slices of the two different 3D structures considered for the study. (a) Illustration of a structure generated by the diamond-square fractal process for $d_{\rm frac} = 26$ m. (b) Illustration of a structure corresponding to spheres with a diameter $d_{\rm sph} = 6$ m embedded into a homogeneous matrix.

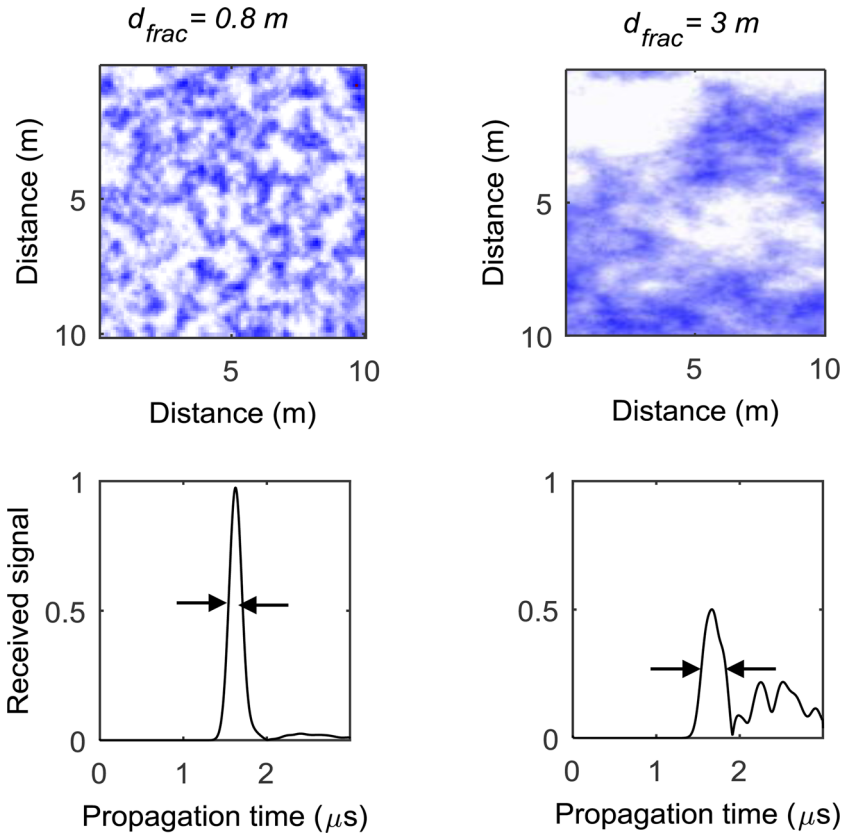

Figure 7. Illustration of the effect of the propagation through a non-homogeneous nucleus on the pulse shape. The shape of the received pulse is shown at the bottom. A 2D slice of each nucleus model considered is represented on the top. Examples obtained with a fractal structure have been chosen for illustrative purposes.

representative characteristics. The results presented in the following sections are the $\Delta T_{\rm 6dB}$ averaged over those 60 simulations.

As an illustration of the effect of volume scattering on the pulse width, Fig. 7 shows the pulse shape obtained by simulation for two different nucleus structures generated with the diamond-square method. The model with the smallest structures ($d_{\rm frac} = 0.8$ m) produces almost no scattering hence no pulse broadening while the model corresponding to a larger characteristic size ($d_{\rm frac} = 3$ m) gives a broader pulse and, concurrently, a weaker amplitude due to volume scattering. The spheres model would give the very same behaviour.

4.3.1 Effect of variable dielectric permittivity contrast $\Delta\varepsilon$ simulated over a distance of 200 m

Due to Philae's bouncing at the surface after its touch-down, the final position of Philae was not the one expected. As a consequence, no measurement have been performed at grazing angles and the smallest travelled distance inside the nucleus L is around 200 m for both $FSS_{\rm West}$ and $FSS_{\rm East}$. If any volume scattering is to be expected, the impact on the pulse width should be increasing with L. The results obtained for $L = 200$ m provide a first cut that allows to restrict the heterogeneities size and permittivity contrast values compatible with the CONSERT data.

Downloaded from https://academic.oup.com/mnras/article/469/Suppl_2/S805/4705912 by guest on 11 November 2020

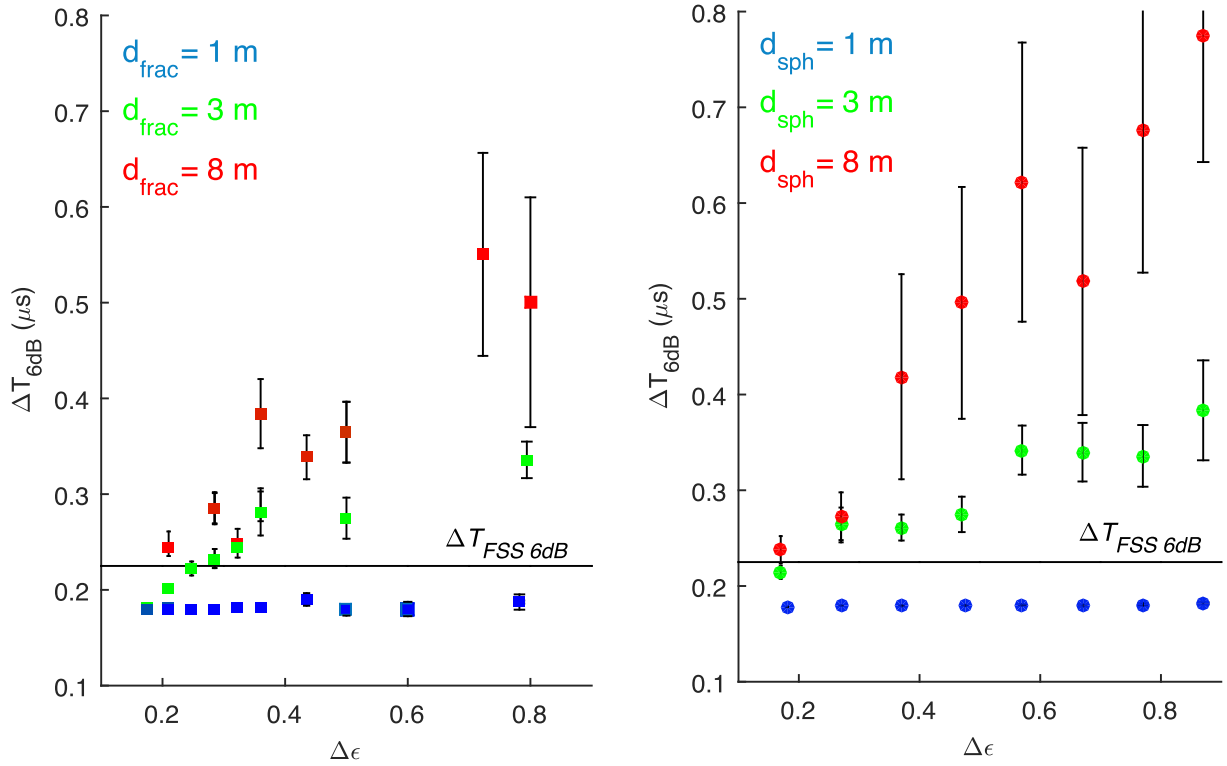

Figure 8. Pulse width at 6 dB versus the permittivity contrast $\Delta\varepsilon$ for three sizes of heterogeneities with the fractal model (left) and with the spheres model (right). The travelled distance is $L = 200$ m. The experimental threshold values $\Delta T_{FSS\ 6dB}$ is represented by the solid horizontal line.

Fig. 8 shows the pulse width values as a function of the permittivity contrast for three different sizes of heterogeneities with the corresponding error bars. The variability of the computed pulse width increases with the heterogeneities scale because for larger scale the behaviour becomes less representative of the statistical parameters chosen for the nucleus model. The same behaviour can be observed for the two nucleus models considered: For $d_{\rm sph} \leq 1$ m or $d_{\rm fra} \leq 1$, whatever the permittivity contrast is, the pulse width remains equal to the one that would correspond to a perfectly homogeneous nucleus. The broadening of the pulse due to volume scattering is noticeable for the larger spatial scale and increasing with the permittivity contrast for both models, even if the effect is more noticeable for the spheres model. For the two nucleus structures we consider, the measurements corresponding to a travelled length of 200 m are not compatible with a permittivity contrast $\Delta\varepsilon$ larger than 0.25 unless the heterogeneities size is around 1 m.

4.3.2 Effect of the distance travelled inside the material at a given dielectric permittivity contrast $\Delta\varepsilon$ simulated

We now focus on the effect of the distance travelled inside the nucleus for a permittivity contrast of 0.25, which is the highest value that might be compatible with CONSERT's observation for structures that have a few metres spatial scale. The results are shown on Fig. 9 for the spheres model and for the diamond-square model. As expected the volume scattering effect becomes more visible when the distance travelled inside the material increases. Once again the effect would be more noticeable for the spheres model. But for both models, we can conclude that the CONSERT's wave did not propagate for more than 200 m inside a nucleus presenting heterogeneities of a few metres size with a permittivity contrast higher than 0.25.

4.4 Discussion and interpretation

Based on the comparison between experimental data collected by CONSERT during the FSS and simulation results, we obtain the following constraints on the physical properties of the cometary material inside the sounded part of the small lobe:

(1) For both structural models we considered, if the size of the heterogeneities is smaller than 1 m, then any contrast of permittivity at least up to 1 and whatever the distance of propagation through the nucleus, the model would be consistent with the measured data. Such a permittivity contrast would be observed for example between vacuum (permittivity equal to 1) and pure CO_2 ice (permittivity around 2.1), pure refractory carbon (permittivity around 2) or any mixture of material with higher intrinsic permittivity values (i.e. water ice and dust) with the right amount of porosity.

(2) Should there be heterogeneities of the order of 3 m, like the potential cometesimals detected on the surface of 67P/C-G described in Section 2.2, then the permittivity contrast should necessarily be below 0.25 otherwise the width of the CONSERT signal would have been affected to a measurable extent. This maximum permittivity contrast value of 0.25, compatible with CONSERT's observations, is rather low which is consistent with a high porosity inside the nucleus. It could be explained by a difference in porosity or/and in composition. Based on the model of permittivity and composition developed in Hérique et al. (2016), such a difference would most likely be explained by local changes in porosity rather than by local changes in the composition. This permittivity contrast could correspond to a nucleus with highly porous areas (>95 per cent, i.e. voids) and with areas having a porosity around 60 per cent. On the other hand, if we consider a uniform porosity of 75 per cent inside the sounded part of the nucleus, a local variation of the dust

Downloaded from https://academic.oup.com/mnras/article/469/Suppl_2/S805/4705912 by guest on 11 November 2020

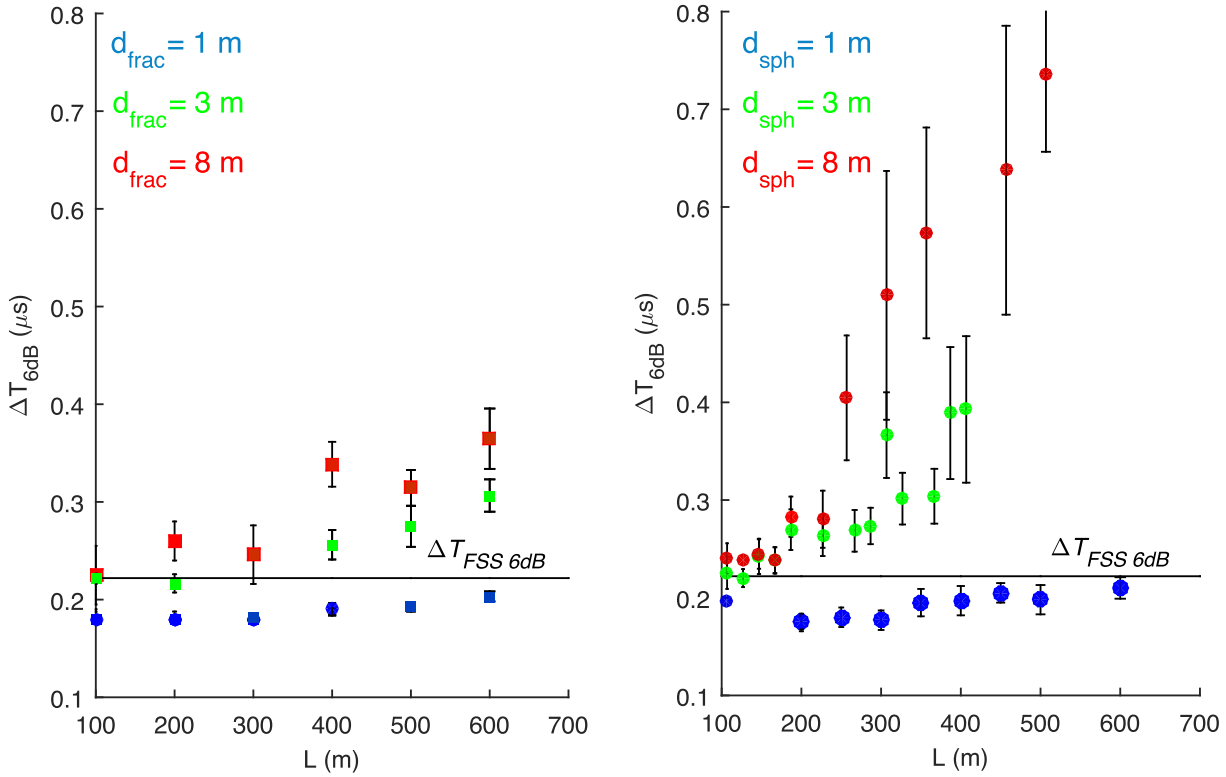

Figure 9. Pulse width at 6 dB versus distance travelled inside a non-homogeneous nucleus for the sphere model (left) and for the fractal model (right) a permittivity contrast of 0.25. The experimental threshold values $\Delta T_{FSS\ 6dB}$ is represented by the solid horizontal line.

to ice ratio would correspond to contrast lower than 0.25 and would thus be compatible with CONSERT's data.

In other words, these combinations of values (i.e. a typical size around 1 m with a permittivity contrast up to 1 and a typical size around 3 m with a permittivity contrast lower than 0.25) constitute the limit of sensitivity of our analysis of the CONSERT data. The absence of any pulse spreading due to scattering allows us to exclude heterogeneity with higher contrast and larger size (but remaining on the few wavelengths scale, since larger scales can be responsible for multipath propagation). It is important to note that simulations with two very different models lead to the same interpretation for the measurements, illustrating the robustness of the conclusions derived by the method.

5 CONCLUSION

Because its activity periodically resurfaces its nucleus, any clue about the formation processes of 67P/C-G have to be inferred from physical properties of the material at depth. CONSERT's instrument has been specifically designed to sound the internal structure of the nucleus. Since CONSERT is a radar, the information it can provide is linked to the dielectric properties of the sounded materials, which needs then to be interpreted in terms of composition and porosity.

During FSS, CONSERT's electromagnetic waves successfully travelled through parts of the small lobe of comet 67P/C-G over distances ranging from 200 to at least 900 m. The measured propagation delays allowed to retrieve an averaged value of the dielectric permittivity 1.27 ± 0.05 (Kofman et al. 2015), which corresponds to a wavelength of 3 m in the nucleus. In this paper, we focus on the waveform of the received signal, which provides information about a potential heterogeneity inside the nucleus at a spatial scale commensurate with the wavelength. Studying the nucleus structure at 3-m spatial scale is important because it is the typical size of boulders seen at the surface and, above all, of the structures that are seen on the walls of the pits and have been argued to represent a signature of the primordial building blocks of 67P/C-G.

The parameter used to characterize the received pulses' shape is the pulse width computed at 3 and 6 dB below the maximum amplitude of the pulse. This parameter values have been computed for the FSS sequence (whenever the quality of the CONSERT's signal was good enough) and compared to a reference value experimentally obtained with the spare model of the instrument's electronics on Earth. The experimental values obtained during FSS show a slight but not significant increase with respect to the reference values. Moreover, there is no sizeable effect of the distance travelled inside the nucleus. These observations are consistent with the fact that no significant volume scattering is taking place during the wave propagation, which means that, from a dielectric point of view, the nucleus is fairly homogeneous at the wavelength scale.

3D electromagnetic simulations have been run on a series of non-homogeneous nucleus models. Two different models have been used to generate these nuclei. The first structure is based on spherical inclusions and accretion in a homogeneous matrix whose electrical properties are very close to the vacuum ones. The second structure is generated by the so-called diamond-square band-limited fractal process, in line with models of nuclei formation from low density fractal aggregates with irregular shapes and consistent with observations at 67P/C-G's surface. Simulated pulses have been obtained for typical spatial scales of the order of the wavelength in the medium ranging from 0.8 to 8 m.

Comparison with the experimental pulse width values has been used to find constraints of the structures inside the nucleus that would be compatible with CONSERT's data.

Downloaded from https://academic.oup.com/mnras/article/469/Suppl_2/S805/4705912 by guest on 11 November 2020

(1) We show that structures with a typical size smaller than 1 m even with a significant permittivity contrast would not have any effect on the CONSERT's wave form; CONSERT's observations cannot exclude or give constraints on any 1-m scale potential structures.

(2) 3-m size scale structures are compatible with CONSERT's measurements provided that the permittivity contrast of the structure is less than 0.25. Given the high bulk porosity of 75 per cent inside the sounded part of the nucleus' small lobe, a likely model would be obtained by a mixture, at this 3-m size scale, of voids (vacuum) and blobs with material made of ices and dust with a porosity larger than 60 per cent.

In this paper, we exclusively focused on 3D isotropic structures therefore the effect of potential layers has not been considered. A previous study (Ciarletti et al. 2015) has shown that layers presenting a permittivity gradient over a thickness of tens/hundreds of metres would have a significant effect on the path followed by the waves inside the nucleus. But simulations show that they would not have any effect on the pulse shape. Thinner layers could potentially be responsible for internal multiple reflections with propagation delays small enough that they would be responsible for a noticeable pulse broadening. But given the high porosity of the nucleus, we do not expect that the permittivity contrast between these layers would be high enough to allow significant reflections at their interfaces. Therefore, we do not believe that the experimental pulse width values can be used to rule out or confirm the existence of a potential layering inside the nucleus.

On-going studies are dedicated to the accurate modelling of the antenna radiation pattern (taking into account the lander structure and its close environment, as well as the orbiter structure) which is essential to understand the amplitude of the received signals. Simulations focused on the effect of the nucleus shape at grazing angles will be performed too. They will allow us to carefully disentangle the effect of the surface from any effect due to the internal structure of the nucleus and to understand the multiple echoes detected par CONSERT.

ACKNOWLEDGEMENTS

Support from the Centre National d'Etudes Spatiales (CNES, France) for this work, based on observations with CONSERT on board *Rosetta*, is acknowledged. The CONSERT instrument was designed built and operated by IPAG, LATMOS, and MPS and was financially supported by CNES, CNRS, UGA, DLR, and MPS.

Rosetta is an ESA mission with contributions from its Member States and NASA.

Rosetta's Philae lander is provided by a consortium led by DLR, MPS, CNES, and ASI. The authors thank the teams of *Rosetta* (SGS and ESOC) and Philae (LCC and SONC) for making the CONSERT operations possible.

REFERENCES

Agarwal J., Müller M., Reach W. T., Sykes M. V., Boehnhardt H., Grün E., 2010, Icarus, 207, 992
Altwegg K. et al., 2016, Sci. Adv., 2, e1600285
Asphaug E., Benz W., 1996, Icarus, 121, 225
Auger A. et al., 2015, A&A, 583, A35
Belton M. J. S. et al., 2007, Icarus, 187, 332
Bentley M. S. et al., 2016, Nature, 537, 73
Bérenger J.-P., 1994, J. Comput. Phys., 114, 185
Bertaux J.-L., 2015, A&A, 583, A38
Bieler A. et al., 2015, Nature, 526, 7575, 678
Boehnhardt H., 2004, Comets II, 745, 301
Brouet Y. et al., 2016, MNRAS, 462, S89
Capanna et al., 2016, Geophys. Res. Abstracts, 18, EGU2016–4522, EGU General Assembly
Ciarletti V. et al., 2015, A&A, 583, A40
Cochran A. L. et al., 2015, Space Sci. Rev., 197, 9
Davidsson B. J., Gutiérrez P. J., 2005, Icarus, 176, 453
Davidsson B. J. et al., 2016, A&A, 592, A63
Dello Russo N., Vervack R. J., Jr., Weaver H. A., Biver N., Bockelée-Morvan D., Crovisier J., Lisse C. M., 2007, Nature, 448, 172
De Sanctis M. C., Lasue J, Capria M. T., Magni G., Turrini D., Coradini A., 2010, Icarus, 207, 341
Desvoivres E., Klinger J., Levasseur-Regourd A. C., Jones G. H., 2000, Icarus, 144, 172
Donn B. D., 1990, A&A, 235, 441
El-Maarry M. R. et al., 2015, A&A, 583, A26
Engrand C., Maurette M., 1998, Meteorit. Planet. Sci., 33, 565
Fernández Y. R., 2009, Planet. Space Sci., 57, 1218
Filacchione G. et al., 2016, Nature, 529, 368
Flynn G. J., Nittler L. R., Engrand C., 2016, Elements, 12, 177
Fray N. et al., 2016, Nature, 538, 72
Fulle M. et al., 2015, ApJ, 802, L12
Groussin O. et al., 2015, A&A, 583, A36
Grün E. et al., 2016, MNRAS, 462, 220
Hadamcik E., Levasseur-Regourd A.-C., 2016, Planet. Space Sci., 123, 51
Heggy E., Palmer E. M., Kofman W., Clifford S. M., Righter K., Hérique A., 2012, Icarus, 221, 925
Hellyer B., 1970, MNRAS, 148, 383
Hérique A., Rogez Y., Pasquero O. P., Zine S., Puget P., Kofman W., 2015, Planet. Space Sci., 117, 475
Hérique A. et al., 2016, MNRAS, 462(Suppl. 1), S516
Ishiguro M., Usui F., Sarugaku Y., Ueno M., 2009, Icarus, 203, 560
Jessberger E. K., Christoforidis A., Kissel J., 1988, Nature, 332, 691
Johansen A., Oishi J. S., Mac Low M.-M., Klahr H., Henning T., Youdin A., 2007, Nature, 448, 1022
Johansen A., Mac Low M.-M., Lacerda P., Bizzarro M., 2015, Sci. Adv., 1, e1500109
Jorda L. et al., 2016, Icarus, 277, 257
Jutzi M., Asphaug E., 2015, Science, 348, 6241
Kelley M. S., Reach W. T., Lien D. J., 2008, Icarus, 193, 572
Kofman W. et al., 1998, Adv. Space Res., 21, 1589
Kofman W. et al., 2007, Space Science Reviews, 128, 413
Kofman W. et al., 2015, Science, 349, aab0639
Langevin Y., Hilchenbach M., Ligier S. et al., 2016, Icarus, 271, 76
Lasue J., Botet R., Levasseur-Regourd A. C., Hadamcik E., 2009, Icarus, 203, 599
Lasue J., Botet R., Levasseur-Regourd A. C., Hadamcik E., Kofman W., 2011, Icarus, 213, 369
Lethuillier A. et al., 2016, A&A, 591, A32
Levasseur-Regourd A. C., Hadamcik E., Desvoivres E., Lasue J., 2009, Planet. Space Sci., 57, 221
Mandelbrot B. B., 1977, Fractals: Form, Chance and Dimension. W H Freeman and Co
Mannel T., Bentley M. S., Schmied R., Jeszenszky H., Levasseur-Regourd A. C., Romstedt J., Torkar K., 2016, MNRAS, 462(Suppl. 1), S304
Massironi M. et al., 2015, Nature, 526, 402
Miller G. S. P., 1986, Comput. Graph., 20, 4
Morbidelli A., Rickman H., 2015, A&A, 583, A43
Mumma M. J., Charnley S. B., 2011, A&A, 49, 471
Pajola M. et al., 2015, A&A, 583, A37
Pasquero O. P., Herique A., Kofman W., 2017, IEEE Trans. Geosci. Remote Sens., 55, 2225
Pätzold M. et al., 2016, Nature, 530, 63
Plettemeier D. et al., 2016, EGU, 18, 15674
Plettemeier D., Statz C., Hahnel R., Herique A., Rogez Y., Kofman W., Ciarletti V., Jorda L., 2017, Geophys. Res. Abstracts, 19, EGU2017-17889-1

Downloaded from https://academic.oup.com/mnras/article/469/Suppl_2/S805/4705912 by guest on 11 November 2020

Pommerol A. et al., 2015, A&A, 583, A25
Poulet F. et al., 2016, MNRAS, 462, S23
Reach W. T., Vaubaillon J., Kelley M. S., Lisse C. M., Sykes M. V., 2009, Icarus, 203, 571
Richards M. A., 2005, Fundamentals of Radar Signal Processing. Tata McGraw-Hill Education
Rickman H. et al., 2015, A&A, 583, A44
Rotundi A. et al., 2015, Science, 347, aaa3905
Rubin M. et al., 2015, Science, 348, 232
Schleicher D. G., Bair A. N., 2011, AJ, 141, 177
Schröder S. E. et al., 2017, Icarus, 285, 263
Sierks H. et al., 2015, Science, 347, aaa1044
Spohn T. et al., 2015, Science, 349, aab0464
Taflove A., Hagness S. C., 2005, Computational Electrodynamics, The Finite Difference Time Domain Method, 3rd edn. Artech House
Thomas N., Alexander C., Keller H. U., 2008, Space Sci. Rev., 138, 165
Thomas N. et al., 2015a, Science, 347, aaa0440
Thomas N. et al., 2015b, A&A, 583, A17
Vincent J.-B. et al., 2015, Nature, 523, 63
Vincent J-B. et al., 2016, A&A, 587, A14
Wahlberg Jansson K., Johansen A., 2015, A&A, 570, A47
Weidenschilling S. J., 2004, Comets II, 745, 97
Weissman P. R., Lowry S. C., 2008, Meteorit. Planet. Sci., 43, 1033
Wright et al., 2015, Science, 349, 6247

SUPPORTING INFORMATION

Supplementary data are available at *MNRAS* online.

Figure S1. One iteration of the diamond-square process on a cubic pattern. For each iterations, eight cubes are generated per pattern.

Please note: Oxford University Press is not responsible for the content or functionality of any supporting materials supplied by the authors. Any queries (other than missing material) should be directed to the corresponding author for the article.

This paper has been typeset from a Microsoft Word file prepared by the author.

Downloaded from https://academic.oup.com/mnras/article/469/Suppl_2/S805/4705912 by guest on 11 November 2020